Interface roughness effects in the giant magnetoresistance in magnetic multilayers

Barnaś, J.; Palasantzas, G.

Published in:
Journal of Applied Physics

DOI:
10.1063/1.365702

Publication date:
1997

Interface roughness effects in the giant magnetoresistance in magnetic multilayers

J. Barnaś[a)]
Unite Mixte de Physique CNRS-Thomson, 91404 Orsay, France and Institute of Physics, A. M. University ul. Matejki 48/49, 60 769 Poznań, Poland

G. Palasantzas[b)]
Delft University of Technology, Dimes Section Submicron Technology, Lorentzweg 1, CJ 2628 Delft, The Netherlands

(Received 17 February 1997; accepted for publication 27 June 1997)

In-plane electronic transport in thin layered magnetic structures composed of two ferromagnetic films separated by a nonmagnetic spacer is analyzed theoretically in the Born approximation. Particular attention is paid to the role of interface roughness in the giant magnetoresistance (GMR) effect. The analysis applies to self-affine interfaces described by the k-correlation model. Our results show that GMR is sensitive to the roughness exponent H $(0 \leqslant H \leqslant 1)$ in a manner that depends on spin asymmetries for bulk and interfacial scattering. The limit of low electron concentration is also considered. © *1997 American Institute of Physics.* [S0021-8979(97)05519-9]

I. INTRODUCTION

When the magnetizations of neighboring magnetic films in an artificially layered metallic magnetic/nonmagnetic structure rotate from antiparallel to parallel alignment, electrical resistivity usually drops by a remarkable factor. This effect is known as the normal giant magnetoresistance (GMR) or spin-valve effect.[1,2] In certain cases, the effect can be inversed; the resistance can increase when the magnetizations rotate from the antiparallel to parallel configuration.[3]

The GMR effect results from two factors: (i) spin dependence of the electronic band structure of a defect-free system, and (ii) spin dependence of scattering potential. In the diffuse limit, the resistivity is determined by scattering processes on impurities and other scattering defects inside the films (bulk scattering), as well as by electron scattering on interfacial roughness. In 3d ferromagnetic films, those scattering processes are usually spin dependent and the spin asymmetry for bulk scattering can be generally different from the spin asymmetry for scattering on rough interfaces. In some cases, the asymmetries for bulk and interfacial scattering can be opposite. By changing parameters which control the ratio of bulk and interfacial contributions to GMR (e.g., by varying film thicknesses, roughness amplitude, impurity concentrations, etc), one can observe either enhancement or suppression of the GMR effect.[4] When the multilayer is asymmetrical in the sense that either bulk or interfacial spin asymmetries in neighboring magnetic films are opposite, one can then induce a transition from the normal to inverse effect (or vice versa).[5]

Much experimental work has been done[6–10] to clarify the role of interface roughness in GMR, but the results are difficult for interpretation and it is still not clear which scattering processes, bulk or interface, give the dominant contribution to the observed effect. Apparently, both contributions are important, but their relative role depends on such factors like quality of interfaces, amount of bulk scattering centers, composition of multilayers, electronic band structure etc.

In various theoretical models, the interfacial roughness was taken into account on different levels. Within the earlier quasiclassical approaches, it was included by some effective phenomenological transmission and reflection coefficients.[11,12] Those coefficients were constant, i.e., independent of the angle of incidence. The model was subsequently improved by Hood *et al.*[13] by including the angle-of-incidence dependence of the transmission and reflection coefficients. A weak point of the quasiclassical description is the fact that interfacial and bulk scattering processes are considered on different levels. Quantum mechanical descriptions, on the other hand, are free of this deficiency.[14–18]

In a recent article, Zhang and Levy[19] showed that detailed microscopic structure of interfaces between ferromagnetic and nonmagnetic layers is crucial for the interfacial contribution to GMR. However, some aspects of the interfacial scattering were still not explored. For example, in most theoretical analyses of the interfacial scattering, the authors considered only the case of uncorrelated interface roughness. The effect of in-plane correlation length ξ on GMR was examined up to now only for the exponential model of the roughness correlation function.[4] In many cases, however, the interfaces can have various fractality degrees, which are described by the roughness exponent H $(0 \leqslant H \leqslant 1)$. The main objective of this article is just theoretical analysis of the role of interface roughness fractality in the GMR effect. The analysis is restricted to those surfaces which can be described by the k-correlation model.[20]

In Sec. II, we describe briefly the model used for theoretical analysis and present appropriate formula for electronic conductivity. Self-affine interfaces are described in Sec. III. In Sec. IV, we consider the case where only a single electron miniband is occupied. Numerical results in a general

[a)]Permanent address: Magnetism Theory Division, Institute of Physics, A. M. University, ul. Matejki 48/49, 60–769 Poznań, Poland.
[b)]Electronic mail: palas@dimes.tudelft.nl

 0021-8979/97/82(8)/3950/7/$10.00

case and final conclusions are presented respectively in Secs. V and VI.

II. DESCRIPTION OF THE MODEL

The model, we assume, is an extension of the model described in Ref. 4 by including self-affine fractal properties of interfaces. Accordingly, we consider two ferromagnetic layers of thicknesses d_1 and d_2, which are separated by a nonmagnetic film of thickness d_0. The two interfaces (indexed in the following with β, $\beta=1,2$) are located at $z=z_\beta+h_\beta(\rho)$, where $z_1=d_1$, $z_2=d_1+d_0$, and ρ is the two-dimensional in-plane position vector. The functions $h_\beta(\rho)$ describe fluctuations from perfectly flat interfaces and are assumed random single-valued functions of the position vector ρ. Generally, both interfaces are described by different correlation functions $C_\beta(\rho)=\langle h_\beta(\rho)h_\beta(0)\rangle$, rms roughness amplitudes $\Delta_\beta=\langle h_\beta^2\rangle^{1/2}$ (with $\langle h_\beta\rangle=0$ by definition) and in-plane correlation lengths ξ_β. For simplicity, the outer surfaces (at $z=0$ and $z=d_1+d_0+d_2\equiv L$, with L the total thickness of the structure) are assumed perfectly flat.

Following Refs. 4 and 21, the zero-temperature global in-plane conductivity g for a colinear (parallel or antiparallel) configuration is given in the Born approximation by the formula

$$g=\frac{e^2\hbar^3}{2m^2L}\sum_\sigma\sum_{\mu=1}^{N_\sigma}\sum_{\mu'=1}^{N_\sigma}Q_{\mu\sigma}^2Q_{\mu'\sigma}^2[\mathbf{C}_\sigma^{-1}(E_F)]_{\mu\mu'}, \quad (1)$$

where μ and μ' index electronic two-dimensional minibands, and N_σ is the number of occupied minibands for spin σ. Apart from this, $Q_{\mu\sigma}$ is the in-plane Fermi wavevector corresponding to the miniband μ and spin σ, while the matrix elements $[\mathbf{C}_\sigma(E_F)]_{\mu\mu'}$ are calculated at the Fermi energy E_F and are given by the expression

$$[\mathbf{C}_\sigma(E_F)]_{\mu\mu'}=\delta_{\mu\mu'}Q_{\mu\sigma}^2\sum_{\nu=1}^{N_\sigma}P_{\mu\nu}^\sigma-Q_{\mu\sigma}Q_{\mu'\sigma}T_{\mu\mu'}^\sigma, \quad (2)$$

where $P_{\mu\nu}^\sigma$ and $T_{\mu\nu}^\sigma$ are defined as

$$P_{\mu\nu}^\sigma=2\pi\sum_{\alpha=0}^{2}n_\alpha v_{\alpha\sigma}^2K_{\alpha\sigma}^{\mu\nu}+\sum_{\beta=1}^{2}[(V_{\beta\sigma}^{(1)})^2+(V_{\beta\sigma}^{(2)})^2]L_{\beta\sigma}^{\mu\nu}(F_{\beta\sigma}^{(1)})_{\mu\nu} \quad (3)$$

and

$$T_{\mu\nu}^\sigma=\sum_{\beta=1}^{2}[(V_{\beta\sigma}^{(1)})^2+(V_{\beta\sigma}^{(2)})^2]L_{\beta\sigma}^{\mu\nu}(F_{\beta\sigma}^{(2)})_{\mu\nu}. \quad (4)$$

Here, the matrices $\mathbf{F}_{\beta\sigma}^{(1)}$ and $\mathbf{F}_{\beta\sigma}^{(2)}$ are defined as

$$(F_{\beta\sigma}^{(1)})_{\mu\nu}=\int_0^{2\pi}\langle|h_\beta(Q_{\mu\nu}^\sigma)|^2\rangle d\theta \quad (5)$$

and

$$(F_{\beta\sigma}^{(2)})_{\mu\nu}=\int_0^{2\pi}\langle|h_\beta(Q_{\mu\nu}^\sigma)|^2\rangle\cos\theta d\theta, \quad (6)$$

where $\langle|h(q)|^2\rangle$ is the Fourier transform of the correlation function (see Sec. III), and $Q_{\mu\mu'}^\sigma=(Q_{\mu\sigma}^2+Q_{\mu'\sigma}^2-2Q_{\mu\sigma}Q_{\mu'\sigma}\cos\theta)^{1/2}$. The parameters $L_{\beta\sigma}^{\mu\nu}$ and $K_{\alpha\sigma}^{\mu\nu}$ introduced in Eq. (3) are defined as

$$L_{\beta\sigma}^{\mu\nu}=[\psi_{\mu\sigma}(z_\beta)\psi_{\nu\sigma}(z_\beta)+\tfrac{1}{4}\Delta_\beta^2\psi'_{\mu\sigma}(z_\beta)\psi'_{\nu\sigma}(z_\beta)]^2 \quad (7)$$

and

$$K_{\alpha\sigma}^{\mu\nu}=\int_{d_\alpha}dz\,\psi_{\mu\sigma}^2(z)\psi_{\nu\sigma}^2(z), \quad (8)$$

where $\psi_{\mu\sigma}(z)$ are the wavefunctions corresponding to the miniband edges (discrete energy levels) and $\psi'_{\mu\sigma}(z)$ are their first derivatives. Apart from this, n_α in Eq. (3) is the impurity concentration in the αth layer and $v_{\alpha\sigma}$ is the impurity scattering potential which is spin dependent for the magnetic films ($\alpha=1$ and 2) and independent of the electron spin for the nonmagnetic spacer ($\alpha=0$). Finally, $V_{\beta\sigma}^{(1)}$ is the spin dependent potential step at the βth interface, and $V_{\beta\sigma}^{(2)}$ is an effective potential which takes into account additional interfacial scattering caused by $s-d$ hybridization.[4]

The bulk electron concentrations in constituting materials are determined by the corresponding bulk chemical potentials $\mu_{\alpha\sigma}=\mu-U_{\alpha\sigma}$, where μ is the common chemical potential and $U_{\alpha\sigma}$ is the crystalline electron potential (spin dependent in the magnetic films and $U_{0\sigma}=U_0=0$ in the nonmagnetic spacer). Consequently, the potential steps $V_{\beta\sigma}^{(1)}$ are equal to $U_{\beta\sigma}-U_0$. The Fermi energy E_F in the layered structure is adjusted to keep the system electrically neutral.

In the following, we will use the notation according to which the electron spin projection on the local quantization axis (direction opposite to the local magnetization) is denoted as ''+'' for spin-majority electrons and ''−'' for spin-minority electrons, while spin projection on the global quantization axis by ''↑'' and ''↓.''

As we already mentioned above, the formula (1) was derived in the Born approximation, which imposes some constrains on the applicability range of the derived results. First of all, the roughness amplitude has to be small; significantly smaller than the film thicknesses. Consequently, the dependence of GMR on the roughness amplitude is described properly in this approximation only for small values of the roughness amplitudes. For larger amplitudes, this approximation gives a monotonous increase of GMR,[4] whereas a nonperturbative quasiclassical description gives a maximum of GMR at a certain roughness amplitude.[22]

III. SELF-AFFINE FRACTAL INTERFACES

The correlation function $C(\mathbf{r})$ for any physical self-affine interface is characterized by a finite correlation length ξ, which is a measure of average distance between consecutive peaks and valleys on the interface such that $C(\mathbf{r})\approx\Delta^2-Dr^{2H}$ for $r\ll\xi$ and $C(\mathbf{r})=0$ for $r\gg\xi$ ($D\sim\Delta^2/\xi^{2H}$ is a constant).[20,23–25] The roughness exponent H ($0\leqslant H\leqslant 1$) describes the interface irregularity. Small values of H characterize interfaces which are relatively jugged at short length scales ($r\ll\xi$) but smoother at larger length scales, while

large values of H correspond to interfaces which are smoother at short length scales but more irregular at larger length scales.[20,23,25]

For self-affine fractal interfaces, the Fourier transform $\langle|h(q)|^2\rangle$ of $C(\mathbf{r})$ has the scaling behavior $\langle|h(q)|^2\rangle \sim q^{-2-2H}$ if $q\xi \gg 1$, and $\langle|h(q)|^2\rangle \sim$ const if $q\xi \ll 1$. This scaling behavior in the Fourier space is satisfied by the k-correlation model,[20]

$$\langle|h(q)|^2\rangle = \frac{2\pi\Delta^2\xi^2}{(1+aq^2\xi^2)^{1+H}}. \tag{9}$$

The normalization condition $\int_{0<q<q_c}\langle|h(q)|^2\rangle d^2q = (2\pi\Delta)^2$ yields the following equation for the parameter a: $a=(1/2H)[1-(1+aq_c^2\xi^2)^{-H}]$ for $0<H\leqslant 1$ and $a=(1/2)\ln(1+aq_c^2\xi^2)$ for $H=0$. Here q_c is the upper cut-off in the Fourier space, $q_c=\pi/a_0$, where a_0 is the interatomic spacing (in the following numerical calculations we assume $a_0=3$ Å). Our description of the influence of interface roughness on electronic transport is restricted to those interfaces which obey Eq. (9).

IV. SINGLE OCCUPIED MINIBAND

Equation (1) can be used for numerical calculations of the electronic conductivity g. However, it is rather difficult to obtain from it an analytical expression in a general case. This is due to the following reasons: (i) The discrete energy levels (miniband edges) and the corresponding wavefunctions (consequently also the parameters $K_{\alpha\sigma}^{\mu\nu}$ and $L_{\beta\sigma}^{\mu\nu}$) can be found generally only from numerical calculations.[4] Exact analytical expressions can be obtained only for the case of a uniform electron potential across the structure with infinite external confining potential (simple quantum well). (ii) The integrals in Eqs. (5) and (6) cannot be generally calculated analytically except two special cases of $H=0$ and $H=1$, as described in the Appendix A. (iii) When the number of occupied minibands is large (metallic films or thick semiconductor ones), the inverse matrix in Eq. (1) can be calculated only numerically.

In this section, we consider a simple case, where only a single miniband is occupied by electrons. Such a situation may occur in magnetic semiconductor trilayers. In that case, Eq. (1) leads to the following expression for the electronic conductivity:

$$g = \frac{e^2\hbar^3}{2m^2L}\sum_{\sigma(=\uparrow,\downarrow)}\frac{Q_\sigma^2}{\Phi_\sigma^{\mathrm{imp}}+\Phi_\sigma^{\mathrm{int}}}, \tag{10}$$

where $Q_\sigma \equiv Q_{1\sigma}$, and

$$\Phi_\sigma^{\mathrm{imp}} = 2\pi\sum_{\alpha=0}^{2} n_\alpha v_{\alpha\sigma}^2 K_{\alpha\sigma} \tag{11}$$

and

$$\phi_\sigma^{\mathrm{int}} = \sum_{\beta=1}^{2}[(V_{\beta\sigma}^{(1)})^2+(V_{\beta\sigma}^{(2)})^2]L_{\beta\sigma}F_{\beta\sigma}. \tag{12}$$

For bravity of notation, the indices $\mu=1$ and $\nu=1$ at $K_{\alpha\sigma}^{\mu\nu}$ and $L_{\beta\sigma}^{\mu\nu}$ have been omitted, $K_{\alpha\sigma}\equiv K_{\alpha\sigma}^{11}$ (for $\alpha=0$, 1, and 2) and $L_{\beta\sigma}\equiv L_{\beta\sigma}^{11}$ (for $\beta=1$ and 2). Apart from this, $F_{\beta\sigma}$ in Eq. (12) is defined as

$$F_{\beta\sigma} = (F_{\beta\sigma}^{(1)})_{11}-(F_{\beta\sigma}^{(2)})_{11} = \int_0^{2\pi}\langle|h_\beta(\widetilde{Q}_\sigma)|^2\rangle(1-\cos\theta)d\theta, \tag{13}$$

where $\widetilde{Q}_\sigma \equiv Q_{11\sigma} = Q_\sigma\sqrt{2(1-\cos\theta)}$.

When the electronic potential is uniform (and consequently independent of the spin direction), all the quantities Q_σ, $\widetilde{Q}_\sigma$, $K_{\alpha\sigma}$, $L_{\beta\sigma}$, and $F_{\beta\sigma}$ are independent of the spin direction. Droping the spin index, one can rewrite Eq. (10) as

$$g = \frac{e^2\hbar^3}{2m^2L}\,Q^2\sum_{\sigma(=\uparrow,\downarrow)}\frac{1}{\Phi_\sigma^{\mathrm{imp}}+\Phi_\sigma^{\mathrm{int}}}, \tag{14}$$

with

$$\Phi_\sigma^{\mathrm{imp}} = 2\pi\sum_{\alpha=0}^{2} n_\alpha v_{\alpha\sigma}^2 K_\alpha \tag{15}$$

and

$$\Phi_\sigma^{\mathrm{int}} = \sum_{\beta=1}^{2}(V_{\beta\sigma}^{(2)})^2 L_\beta F_\beta. \tag{16}$$

In Eq. (16), we took into account the fact that now the potential steps $V_{\beta\sigma}^{(1)}$ vanish. The functions K_α and L_α are given by simple analytical formula, which can be easily found by taking into account Eqs. (7) and (8) and the explicit form of the wavefunction corresponding to the lowest miniband. Their explicit forms are given in Appendix B.

From Eq. (14) follows that the magnetoresistance, defined as the ratio $\Delta\rho/\rho_p=(\rho_{\mathrm{AP}}-\rho_P)/\rho_P$, where ρ_{AP} and ρ_P are the resistivities, respectively, in the antiparallel and parallel configurations, is given by the formula

$$\frac{\Delta\rho}{\rho_P} = \frac{(\Phi_{\sigma\mathrm{AP}}^{\mathrm{imp}}+\Phi_{\sigma\mathrm{AP}}^{\mathrm{int}})(\Phi_{-\sigma\mathrm{AP}}^{\mathrm{imp}}+\Phi_{-\sigma\mathrm{AP}}^{\mathrm{int}})}{(\Phi_{\sigma P}^{\mathrm{imp}}+\Phi_{\sigma P}^{\mathrm{int}})(\Phi_{-\sigma P}^{\mathrm{imp}}+\Phi_{-\sigma P}^{\mathrm{int}})}-1, \tag{17}$$

where $\Phi_{\sigma P}^{\mathrm{imp}}$ and $\Phi_{\sigma\mathrm{AP}}^{\mathrm{imp}}$ ($\Phi_{\sigma P}^{\mathrm{int}}$ and $\Phi_{\sigma\mathrm{AP}}^{\mathrm{int}}$) are given by Eq. (15) [Eq. (16)], respectively, for the parallel and antiparallel configurations of the film magnetizations. In the following, we will consider the limiting cases of dominant bulk and interface scattering.

(A) Bulk scattering dominates, so the interfacial scattering can be neglected. Equation (17) leads then to the following formula for the magnetoresistance

$$\frac{\Delta\rho}{\rho_P}=\frac{K_1K_2(\rho_{1+}-\rho_{1-})(\rho_{2+}-\rho_{2-})}{(K_1\rho_{1+}+K_0\rho_0+K_2\rho_{2+})(K_1\rho_{1-}+K_0\rho_0+K_2\rho_{2-})}, \tag{18}$$

where $\rho_{1\pm}$ and $\rho_{2\pm}$ are the corresponding bulk resistivities for majority $(+)$ and minority $(-)$ electrons in both magnetic films, and ρ_0 is the resistivity (per spin) of the nonmagnetic spacer. K_1, K_0, and K_2 take into account quantum size effects and the effects due to different film thicknesses. Their analytical forms are given in Appendix B.

When the structure is symmetrical ($K_1=K_2\equiv K$, $\rho_{1\pm}=\rho_{2\pm}\equiv\rho_{\pm}$), Eq. (18) reduces to the following one

$$\frac{\Delta\rho}{\rho_P}=\frac{(1-\alpha)^2}{4(1+\eta\delta/2)(\alpha+\eta\delta/2)}, \tag{19}$$

where $\alpha=\rho_-/\rho_+$, $\eta=K_0/K$ and $\delta=\rho_0/\rho_+$.

(B) Interfacial scattering dominates and the bulk scattering is ignored. Equation (17) gives then

$$\frac{\Delta\rho}{\rho_P}=\frac{L_1L_2F_1F_2[(V_{1+}^{(2)})^2-(V_{1-}^{(2)})^2][(V_{2+}^{(2)})^2-(V_{2-}^{(2)})^2]}{[L_1F_1(V_{1+}^{(2)})^2+L_2F_2(V_{2+}^{(2)})^2][L_1F_1(V_{1-}^{(2)})^2+L_2F_2(V_{2-}^{(2)})^2]}. \tag{20}$$

For arbitrary roughness exponents, the functions F_1 and F_2 can be calculated only numerically. Analytical forms can be obtained in the case of $H=0$ and $H=1$, as shown in Appendix A.

Generally, both interfaces are described by different values of the rms roughness amplitudes Δ_β and correlation lengths ξ_β. The corresponding roughness exponents H_β can also be different, $H_1\neq H_2$. In that case, magnetoresistance is given by Eq. (20). When, however, $\xi_1=\xi_2\equiv\xi$ and $H_1=H_2\equiv H$, then Eq. (20) reduces to to the following one

$$\frac{\Delta\rho}{\rho_P}=\frac{L_1L_2\Delta_1\Delta_2[(V_{1+}^{(2)})^2-(V_{1-}^{(2)})^2][(V_{2+}^{(2)})^2-(V_{2-}^{(2)})^2]}{[L_1\Delta_1(V_{1+}^{(2)})^2+L_2\Delta_2(V_{2+}^{(2)})^2][L_1\Delta_1(V_{1-}^{(2)})^2+L_2\Delta_2(V_{2-}^{(2)})^2]}, \tag{21}$$

and the magnetoresistance neither depends on the correlation length ξ nor the roughness exponent H.

Numerical results in the case when $H_1\neq H_2$ are shown in Fig. 1, where GMR is plotted as a function of H_1 for a constant value of H_2 ($H_2=0.5$) and for $\xi_1=\xi_2\equiv\xi$. Different curves correspond to different values of ξ and for all ξ GMR increases with increasing H. However, for $H_1=H_2$, all the curves cross at the same point, in agreement with the formula (21).

Figure 2 corresponds to the case where $H_1=H_2\equiv H$, while $\xi_1\neq\xi_2$. GMR is plotted there as a function of H and different curves correspond to different values of ξ_1, while ξ_2 is constant. For $\xi_1=20$ Å ($\xi_1=\xi_2$), the magnetoresistance is independent of H, in agreement with Eq. (21).

For a symmetrical structure with conferral interfaces ($L_1=L_2$, $F_1=F_2$ and $V_{1\pm}^{(2)}=V_{2\pm}^{(2)}\equiv V_{\pm}^{(2)}$), Eq. (20) reduces to the following simple relation:

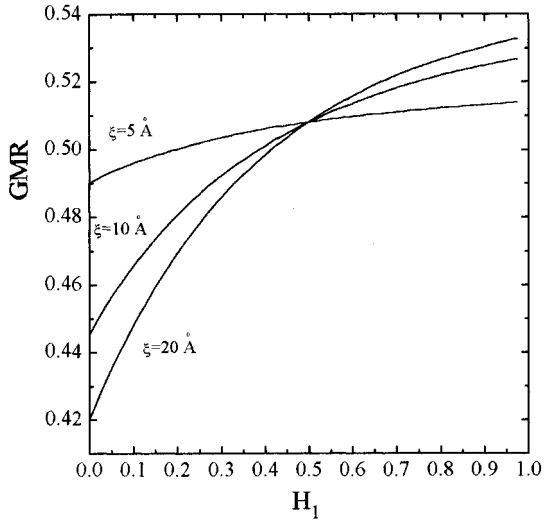

FIG. 1. Magnetoresistance ($\Delta\rho/\rho_P$) plotted as a function of the roughness exponent H_1 for the constant value of $H_2=0.5$ and for $\xi_1=\xi_2\equiv\xi$, with ξ as indicated. The other parameters assumed here are: $d_1=d_0=15$ Å, $d_2=20$ Å, $V_{1+}^{(2)}=V_{2+}^{(2)}=0.5$ eV, $V_{1-}^{(2)}=V_{2-}^{(2)}=1$ eV, and $\Delta_1=\Delta_2=2$ Å. The areal electron concentration was assumed to be equal to 4×10^{-4} Å^{-2}.

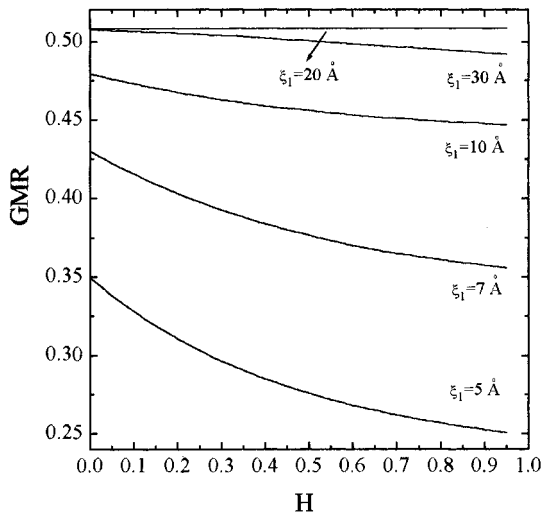

FIG. 2. Magnetoresistance ($\Delta\rho/\rho_P$) as a function of the roughness exponent $H(H_1=H_2\equiv H)$ for $\xi_2=20$ Å and for ξ_1 as indicated. The other parameters are the same as in Fig. 1.

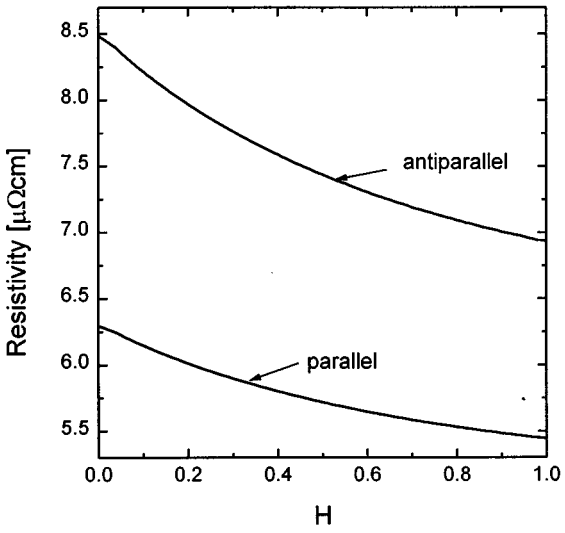

FIG. 3. Resistivity as a function of the roughness exponent $H(H=H_1=H_2)$ in the parallel and antiparallel configurations, calculated for $d_1=d_2=20$ Å, $d_0=15$ Å, $\mu=3$ eV, $U_{1+}=U_{2+}=0.5$ eV, $U_{1-}=U_{2-}=1$ eV, $V_{1\pm}^{(2)}=V_{2\pm}^{(2)}=0$, $\lambda_{1+}=\lambda_{2+}=600$ Å, $\lambda_{1-}=\lambda_{2-}=200$ Å, $\lambda_0=500$ Å, $\Delta_1=\Delta_2=2$ Å, and $\xi_1=\xi_2=5$ Å.

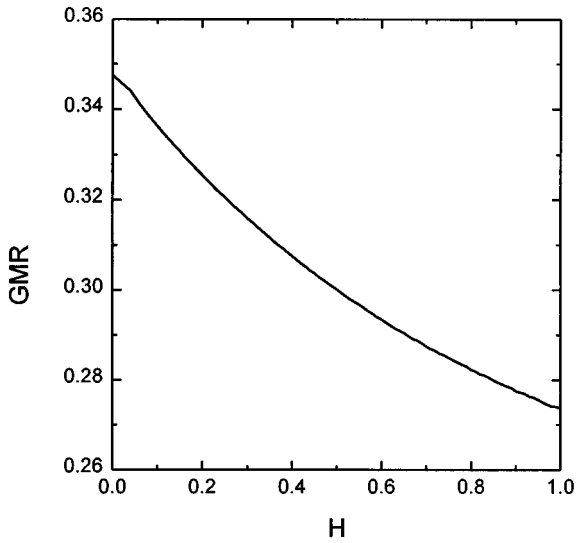

FIG. 4. Magnetoresistance $(\Delta\rho/\rho_P)$ corresponding to the situation shown in Fig. 3.

$$\frac{\Delta\rho}{\rho_P}=\frac{(1-\gamma)^2}{4\gamma}, \tag{22}$$

where $\gamma=(V_-^{(2)}/V_+^{(2)})^2$. As follows from the above formula, the magnetoresistance is then independent of the roughness and is determined only by the spin asymmetry of the scattering potential. Equations (19) and (22) are equivalent to the corresponding formulas given by Levy.[26]

V. NUMERICAL RESULTS FOR METALLIC TRILAYERS

Consider now a metallic sandwich (large N_σ) with spin dependent potentials $U_{\alpha\sigma}$ and $v_{\alpha\sigma}$ in the ferromagnetic films. In the following, electron scattering on impurities will be described quantitatively by the corresponding electron mean free paths, i.e., $\lambda_{\alpha\pm}$ for spin-majority $(+)$ and spin-minority $(-)$ electrons in the ferromagnetic films ($\alpha=1$ and 2), and λ_0 in the spacer layer. Apart from this, we assume that both interfaces ($\beta=1$ and 2) scatter electrons only via the component $V_{\beta\sigma}^{(1)}$, while $V_{\beta\sigma}^{(2)}=0$ for both values of σ.

Assume first, the case when both bulk and interfacial spin asymmetries are of the same kind. This means that both scattering potentials scatter more effectively the same sort of electrons (either majority or minority). Figures 3 and 4 show, respectively, the resistivities in both configurations and the corresponding magnetoresistance as a function of the roughness exponent H (assumed the same for both interfaces). For both parallel and antiparallel configurations, the resistivities decrease with increasing H. This is a consequence of the fact that small values of H correspond to more irregular interfaces at short length scales, which leads to stronger scattering. The corresponding magnetoresistance (Fig. 4) also decreases with increasing H.

Consider now the situation when the bulk and interfacial spin asymmetries are opposite, i.e., if e.g., spin-majority electrons are scattered more effectively by impurities, they are subject to a weaker interfacial scattering potential than the minority electrons. Figures 5 and 6 show, respectively, the resistivities and magnetoresistance. As before, the resistivities decrease with increasing H. The magnetoresistance, however, first decreases with increasing H and then, after reaching a minimum, increases with a further increase of H. This behavior results from an interplay of both bulk and interfacial contributions to the GMR effect.

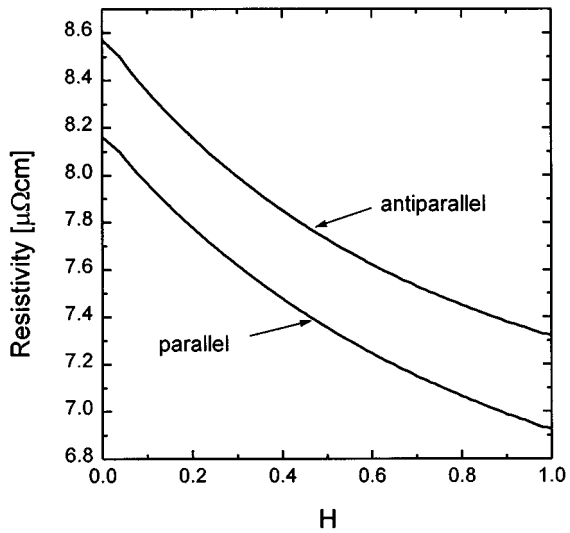

FIG. 5. Resistivity as a funciton of $H(H=H_1=H_2)$ for parallel and antiparallel alignment, calculated for the same parameters as in Fig. 2, except electron mean free paths $\lambda_{1\pm}$ and $\lambda_{2\pm}$, which now have opposite spin asymmetry; $\lambda_{1+}=\lambda_{2+}=200$ Å and $\lambda_{1-}=\lambda_{2-}=600$ Å.

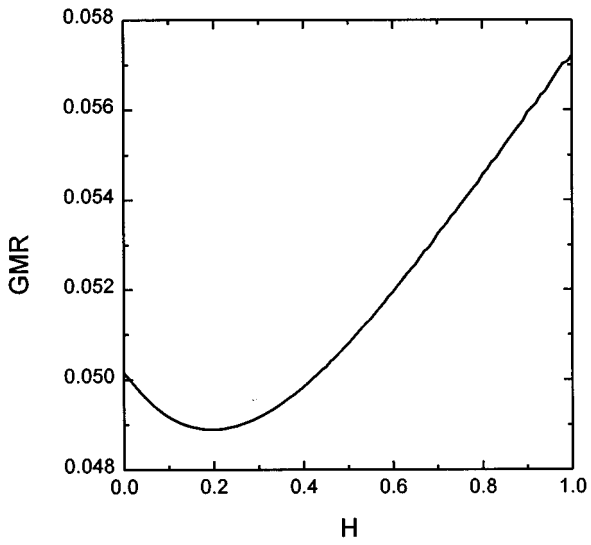

FIG. 6. Magnetoresistance ($\Delta\rho/\rho_P$) corresponding to the situation shown in Fig. 5.

VI. SUMMARY

We have analyzed the role of interfacial roughness in the GMR effect. The resistivities and MR were calculated as a function of the following parameters: (i) rms roughness amplitude, in-plane roughness correlation length, and roughness exponent. Particular attention was paid to the interface fractality effects in GMR. When the spin asymmetry for bulk scattering processes is of the same kind as for interface scattering, then both contributions add constructively to GMR. In that case, GMR varies monotonously with increasing roughness exponent H. When, however, the spin asymmetries for bulk and interfacial scattering are opposite, magnetoresistance varies in a more complex way with increasing H, having generally an extremum at some value of the roughness exponent.

In the calculations described above, the effect of roughness exponent H on GMR was considered in the whole range, $0 \leqslant H \leqslant 1$. Although one might expect contributions from dimensions of the order of a few lattice spacings, which might imply that large values of H ($H \sim 1$) are unphysical, recent studies on Au/NiCo/Au multilayers indicate possible roughness exponent also in the range of $0.7 \leqslant H \leqslant 1$.[27]

ACKNOWLEDGMENTS

J.B. acknowledges hospitality at the Unite Mixte de Physique CNRS-Thomson and also support through the Research Project 8T11F01509 of the Polish Research Committee. G.P. acknowledges hospitality at the Department of Applied Physics (Nanophysics Group) of the Delft University.

APPENDIX A

For $H=0$ and $H=1$, the integrals in Eqs. (5) and (6) can be calculated analytically. Let us suppress the interface index β and define the following parameters

$$\Gamma^{\sigma}_{\mu\mu'} = 1 + a\xi^2 (Q^2_{\mu\sigma} + Q^2_{\mu'\sigma}), \tag{23}$$

$$B^{\sigma}_{\mu\mu'} = 2aQ_{\mu\sigma}Q_{\mu'\sigma}\xi^2 (\Gamma^{\sigma}_{\mu\mu'})^{-1}, \tag{24}$$

where the parameter a is a function of the roughness exponent (see Sec. III).

For $H=0$, Eqs. (5) and (6) lead to the following expressions

$$(F^{(1)}_{\sigma})_{\mu\mu'} = (2\pi\Delta\xi)^2 (1+\Gamma^{\sigma}_{\mu\mu'})^{-1} [1-(B^{\sigma}_{\mu\mu'})^2]^{-1/2} \tag{25}$$

and

$$(F^{(2)}_{\sigma})_{\mu\mu'} = \frac{(2\pi\Delta\xi)^2}{B^{\sigma}_{\mu\mu'}} (1-(1+\Gamma^{\sigma}_{\mu\mu'})^{-1} \times [1-(B^{\sigma}_{\mu\mu'})^2]^{-1/2}). \tag{26}$$

For $H=1$ (logarithmic roughness), one finds

$$(F^{(1)}_{\sigma})_{\mu\mu'} = (2\pi\Delta\xi)^2 \frac{B^{\sigma}_{\mu\mu'}}{(1+\Gamma^{\sigma}_{\mu\mu'})^2} ([1-(B^{\sigma}_{\mu\mu'})^2]^{-1/2} + B^{\sigma}_{\mu\mu'}[1-(B^{\sigma}_{\mu\mu'})^2]^{-3/2}) \tag{27}$$

and

$$(F^{(2)}_{\sigma})_{\mu\mu'} = (2\pi\Delta\xi)^2 \frac{B^{\sigma}_{\mu\mu'}}{(1+\Gamma^{\sigma}_{\mu\mu'})^2} [1-(B^{\sigma}_{\mu\mu'})^2]^{-3/2}. \tag{28}$$

For a single occupied miniband, the above expressions lead to

$$F_{\sigma} \equiv (F^{(1)}_{\sigma})_{11} - (F^{(2)}_{\sigma})_{11} = (2\pi\Delta\xi)^2 \left(\frac{1}{1+\Gamma_{\sigma}} \sqrt{\frac{1+B_{\sigma}}{1-B_{\sigma}}} - \frac{1}{B_{\sigma}} \right) \tag{29}$$

for $H=0$, and

$$F_{\sigma} \equiv (F^{(1)}_{\sigma})_{11} - (F^{(2)}_{\sigma})_{11} = (2\pi\Delta\xi)^2 \frac{1}{(1+\Gamma_{\sigma})^2} \frac{B^2_{\sigma}}{(1+B_{\sigma})\sqrt{1-B^2_{\sigma}}} \tag{30}$$

for $H=1$. Here Γ_{σ} and B_{σ} are defined as

$$\Gamma_{\sigma} = 1 + 2a\xi^2 Q^2_{\sigma}, \tag{31}$$

$$B_{\sigma} = 2aQ^2_{\sigma}/\Gamma_{\sigma}, \tag{32}$$

with the corresponding value of the parameter a.

APPENDIX B

Taking into account the explicit form of the wavefunction corresponding to the lowest miniband in a simple quantum well and the definitions (7) and (8), one finds

$$K_{\alpha} = \frac{1}{(2L)^2} \left(\frac{\sin(4kd_{\alpha})}{2k} - 4\frac{\sin(2kd_{\alpha})}{k} + 6d_{\alpha} \right) \tag{33}$$

for $\alpha=1$ and $\alpha=2$, and

$$K_0 = \frac{3}{2L} - K_1 - K_2. \tag{34}$$

Similarly, one finds

$$L_\beta = \left(\frac{2}{L}\right)^2 [\sin^2(kd_\beta) + \tfrac{1}{4}\Delta_\beta^2 k^2 \cos^2(kd_\beta)]^2 \tag{35}$$

for $\beta = 1$ and 2. The wavenumber k in all the above expressions is equal $k = \pi/L$.

[1] M. N. Baibich, J. M. Broto, A. Fert, F. Nguyen van Dau, F. Petroff, P. Etienne, G. Creuzet, A. Friederich, and J. Chazelas, Phys. Rev. Lett. **61**, 2472 (1988).
[2] G. Binasch, P. Grünberg, F. Saurenbach, and W. Zinn, Phys. Rev. B **39**, 4828 (1989).
[3] J. M. George, L. G. Pereira, A. Barthelemy, F. Petroff, L. Steren, J. L. Duvail, A. Fert, R. Loloee, P. Holody, and P. A. Schroeder, Phys. Rev. Lett. **72**, 408 (1994).
[4] J. Barnaś and Y. Bruynseraede, Europhys. Lett. **32**, 176 (1995); Phys. Rev. B **53**, 5449 (1996).
[5] S. Y. Hsu, A. Barthelemy, P. Holody, R. Loloee, P. A. Schroeder, and A. Fert, Phys. Rev. Lett. **78**, 2652 (1997).
[6] For a review see S. S. P. Parkin, in *Ultrathin Magnetic Structures II*, edited by B. Heinrich and J. A. C. Bland (Springer, Berlin 1994), p. 148; A. Fert and P. Bruno, *ibid.*, p. 82.
[7] F. Petroff, A. Barthelemy, A. Fert, P. Etienne, and S. Lequien, J. Magn. Magn. Mater. **93**, 95 (1991).
[8] Y. Obi, K. Takanashi, Y. Mitami, N. Tsuda, and H. Fujimori, J. Magn. Magn. Mater. **104–107**, 1747 (1992).
[9] E. E. Fullerton, D. M. Kelly, J. Guimpel, I. K. Schuller, and Y. Bruynseraede, Phys. Rev. Lett. **68**, 859 (1992).
[10] P. Belien, R. Schad, C. D. Potter, G. Verbanck, V. V. Moshchalkov, and Y. Bruynseraede, Phys. Rev. B **50**, 9957 (1994).
[11] R. E. Camley and J. Barnaś, Phys. Rev. Lett. **63**, 664 (1989); J. Barnaś, A. Fuss, R. E. Camley, P. Grünberg, and W. Zinn, Phys. Rev. B **42**, 8110 (1990).
[12] B. Dieny, J. Phys.: Condens. Matter **4**, 8009 (1992); B. Dieny, Europhys. Lett. **17**, 261 (1992).
[13] R. Q. Hood, L. M. Falicov, and D. R. Penn, Phys. Rev. B **49**, 368 (1994).
[14] P. M. Levy, S. Zhang, and A. Fert, Phys. Rev. Lett. **65**, 1643 (1990); S. Zhang, P. M. Levy, and A. Fert, Phys. Rev. B **45**, 8689 (1992).
[15] H. E. Camblong and P. M. Levy, Phys. Rev. Lett. **69**, 2835 (1992).
[16] H. Hasegawa, Phys. Rev. B **47**, 15 073 (1993); Phys. Rev. B **47**, 15 080 (1993).
[17] Y. Asano, A. Oguri, and S. Maekawa, Phys. Rev. B **48**, 6192 (1993); H. Itoh, J. Inoue, and S. Maekawa, Phys. Rev. B **51**, 342 (1995).
[18] P. B. Visscher, Phys. Rev. B **49**, 3907 (1994).
[19] S. Zhang and P. M. Levy, Phys. Rev. Lett. **77**, 916 (1996).
[20] G. Palasantzas, Phys. Rev. B **48**, 14 472 (1993); Phys. Rev. B **49**, 5785E (1994).
[21] G. Fishman and D. Calecki, Phys. Rev. Lett. **62**, 1302 (1989).
[22] J. Barnaś and Y. Bruynseraede, Thin Solid Films **275**, 148 (1996).
[23] B. B. Mandelbrodt, *The Fractal Geometry of Nature* (Freeman, New York, 1982); F. Family and T. Viscek, *Dynamics of Fracatal Surfaces* (World Scientific, Singapore, 1991).
[24] G. Palasantzas and J. Krim, Phys. Rev. Lett. **73**, 3564 (1994).
[25] G. Palasantzas, Phys. Rev. B **49**, 1740 (1994).
[26] P. M. Levy, Solid State Phys. **47**, 367 (1994).
[27] M. Chladek, V. Valvoda, C. Dorner, C. Holy, and J. Grim, Appl. Phys. Lett. **69**, 1318 (1996).